AEJ
Alexandria Engineering Journal

Application and implementation of a microprocessor-based sensorless switched reluctance motor drive

A. L. Mohamadein, R. A. Hamdy and Khaled H. K. Ahmed
Electrical Eng. Dept., Faculty of Eng., Alexandria University, Alexandria, Egypt

This paper presents the design and implementation of sensorless Switched Reluctance Motor (SRM) using a Personal Computer (PC) as a controller. The flux-linkage / current sensorless method is applied in this work. A prototype SRM is developed employing the stator of an existing three-phase induction motor. The simulation and practical results using a developed non-linear model are presented. Two look-up tables are generated from measured data to simulate the non-linear behavior of the magnetic circuit. Also, the paper presents the contribution of using a PC and the available tools to implement sensorless techniques to a SRM.

تتناول المقالة تصميم وتنفيذ المحرك ذى الممانعة المغناطيسية المتقطعة بدون عناصر إستشعار باستخدم الحاسب الشخصى، كمتحكم، تم إستخدام طريقة التيار والمجال المتشابك فى هذا التصميم. نموذج محرك الممانعة المغناطيسية المتقطعة تم الحصول عليه بعد عمليات تشغيل فى العضو الثابت من محرك حثى ذات ثلاثة أوجة. تتضمن المقالة النتائج النظرية والمعملية، كما تم إستنتاج اثنين من جداول القراءات عن طريق القراءات المقاسة وذلك للاستعانه بهما فى محاكاة سلوك الدائره المغناطيسية الغير خطي. أيضا توضح المقالة كيفية أستخدام الحاسب الشخصى والادوات المتاحه لتنفيذ المحرك ذى الممانعة المغناطيسية المتقطعة بدون عناصر إستشعار.

Keywords: SRM, Sensorless, PC, Modeling, Simulation

1. Introduction

SRMs are gaining wider popularity among variable speed drives. This is due to their simple low-cost construction characterized by the absence of magnets and rotor windings, high level of performance over a wide speed range, and fault tolerant power stage design. Availability and moderate cost of the necessary electronic components make SRM drives a viable alternative to other commonly used motors like BLDC (Brush Less DC), PM synchronous and universal motors for numerous applications. Rotor position sensing is an integral part of the SRM. In addition to improving the reliability, sensorless techniques reduce the overall cost and dimension of the drive. Moreover, in certain applications such as compressors, where the ambient conditions do not allow using external position sensors, sensorless drive is a must.

Several sensorless control methods have been reported over the past decade [1- 12]. The various sensorless methods in the literature can be broadly classified into the following: Hardware intensive methods which require external circuitry for signal injection [1, 2], data intensive methods such as flux integration techniques which demand large look-up tables to store the magnetic characteristics of the SRM [3- 5], model based methods such as state observer [6- 8], signal power measurement [9], inductance model based technique [10], neural networks and fuzzy logic [11,12], which call for a fast microprocessor such as DSP (Digital Signal Processor) with high MIPS (Million Instruction Per Second). The various reported methods suggested have their own merits and demerits depending on their principles of operation. Ideally, it is desirable to have a sensorless scheme, which uses only terminal measurements and does not require additional hardware or memory. In addition, it is desired to have reliable operation over the entire speed and torque ranges while maintaining high resolution and accuracy. This, however, might not be the case for many available sensorless schemes.

The main idea, behind these techniques, stems from the fact that the mechanical time constant of the SRM drive is much larger than

its electrical time constant. Therefore, one can recover the encoded position information that is stored in the form of flux linkage, inductance or back-emf by solving the voltage equation in an active or idle phase.

2. Principle of the proposed method

The SRM is a highly non-linear system. The non-linear behavior of the motor has been measured. This method is called the non-linear modeling method. Based on the measured data, a mathematical model is created. Not only it enables the simulation of the SRM drive system, but also makes the development and implementation of sophisticated algorithms for controlling the SRM feasible [3]. Fig. 1 illustrates the magnetization characteristics for the prototype SRM at different rotor positions. The magnetization characteristic is magnetic flux linkage as a function of the phase current and the rotor position. The influence of the phase current is nonlinear in the aligned position, where saturation effects can take place.

The sensorless method proposed in this paper, is based on the flux-linkage/current characteristics. This method becomes popular among various sensorless methods [3- 5]. Fig. 2 shows a schematic of the basic position estimator blocks.

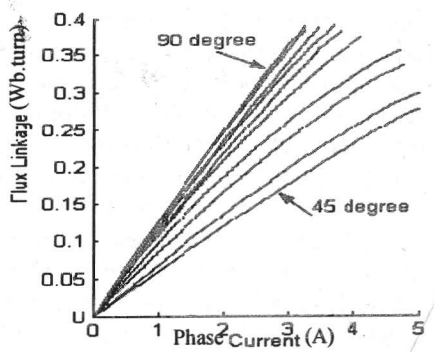

Fig. 1. Flux-Linkage characteristics.

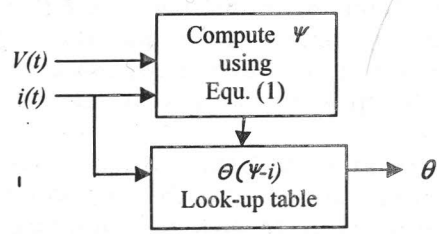

Fig. 2. Schematic of the position estimator.

The magnetization characteristic is firstly measured as the flux-linkage versus current and recorded for different rotor positions. The data is then processed to formulate a look-up table for rotor position as a function of flux linkage and phase current $\theta(\psi,i)$. At any instance, the flux linkage can be calculated by measuring the applied voltage and the phase current as:

$$\Psi = \int (V - ir)\, dt \,. \tag{1}$$

The calculated flux linkage and the measured phase current are then used as inputs to the look-up table $\theta(\Psi\text{-}i)$, to estimate the rotor position.

3. SRM prototype

The stator of a three-phase squirrel cage induction motor is modified to achieve the desired stator saliency for the SRM. The induction motor used comprises 24 slots. For six stator poles, 3-phase SRM the pole pitch spans 60°. Removing one tooth and leaving three the pole arc becomes 37.5°. It should be born in mind that the effective pole arc is still less than the actual pole arc that because of the two slots inside the pole. That is because each stator pole has three teeth and two slots. The rotor comprises 4 poles with 45° pole pitch. Fig. 3 illustrates a schematic that represents the stator and rotor construction. The rated specifications of the machine are:
Phase Voltage = 70 V, Phase Current = 2A,
Torque /phase = 0.19 Nm.

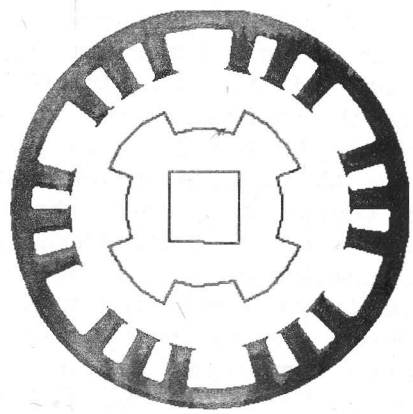

Fig. 3. Construction of the stator and rotor.

4. SRM model

The inherent non-linear nature of the SRM makes the linear model unacceptable. This led to the development of a non-linear model, based on the magnetic characteristics of the SRM. Since only one phase is ON at a time and for simplicity it is assumed that each phase is totally independent of the other phases and the mutual coupling between phases is neglected [5]. This assumption is unacceptable if more than one phase is on and in this case the mutual coupling between phases must be taken into account when building the model.

The dependence of the magnetic characteristics on both the excitation current and the rotor position makes it essential to take the measurements while the phase winding is excited with the appropriate step DC voltage. The phase voltage and current were recorded for different rotor positions. Subtracting the resistive drop and integrating, results in the flux linkage eq. (1). This was done by software integration after data acquisition of the current and voltage. The whole procedure was repeated for different rotor positions. The flux linkage as a function of the phase current and rotor position results in the mesh shown in fig. 4.

Fig. 4 shows that the machine has not gone into saturation for phase current up to 6A. The torque is calculated as the rate of change of magnetic co-energy (W) with respect to rotor displacement as given by eq. (2):

$$T(\theta,i)=\frac{\partial W'(\theta,i)}{\partial\theta}. \qquad (2)$$

The torque data is then interpolated and processed to represent the torque over one rotor pole cycle as a function of rotor position and phase current $T(\theta,i)$, as shown in fig. 5. The notches in the torque surface represent the slots in the stator poles.

Fig. 6, illustrates the torque versus rotor position for three different values of phase current. It is clearly seen that increasing the current, increases the torque. The torque suffers from two notches that become more distinctive at higher currents. This is the result of the fact that the stator pole comprises two slots as mentioned in section 3. It should be noted that higher sampling results in smoother curves.

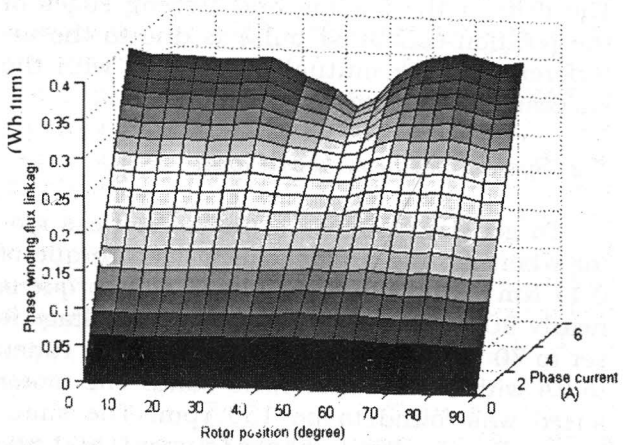

Fig. 4. Flux linkage as a function of the phase current and rotor angle.

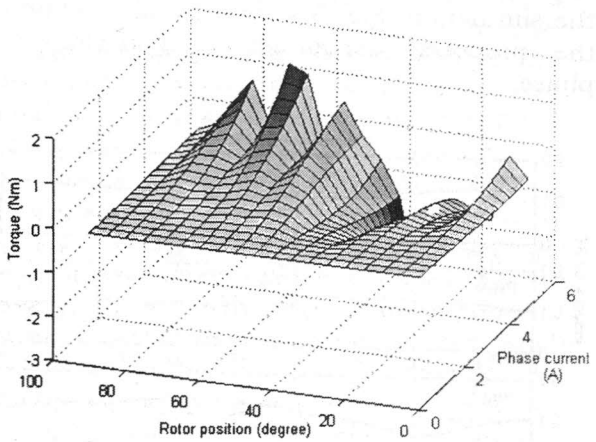

Fig. 5. Torque as a function of rotor position and phase current.

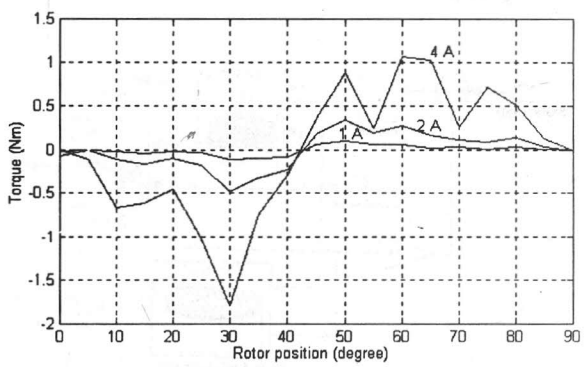

Fig. 6. Torque as a function of rotor position and different phase currents.

The phase inductance was determined from the rate of change of the calculated flux linkage. Fig. 7, illustrates the inductance profile of the three phases as a function of the rotor position at 1A. Fig. 7 shows that phase 1 is aligned at position 0° and unaligned at 45°, the same applies for phase 2 and 3 with 30° phase shift each. It should be born in mind that saturation affects the aligned inductance for higher phase currents. Fig. 4 shows that the motor is not saturated for phase currents up to 6A.

5. Simulation of the proposed sensorless method

In order to understand the dynamics and also to validate the theory of the proposed sensorless scheme, detailed simulations were carried out. The MatLab/ Simulink is used for the simulation. Fig. 8 shows the simulation of the proposed sensorless method for one phase.

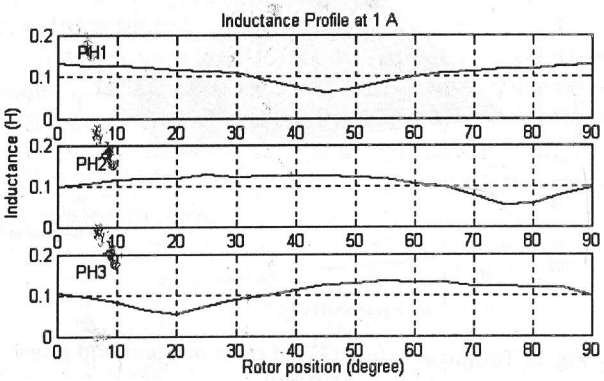

Fig. 7. Inductance profile of the three phase at 1A.

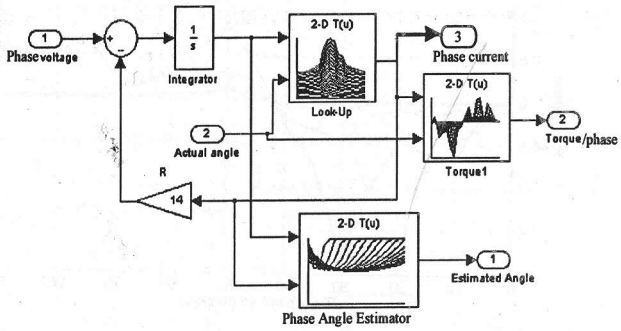

Fig. 8. Block diagram of the simulated senseless method for one phase.

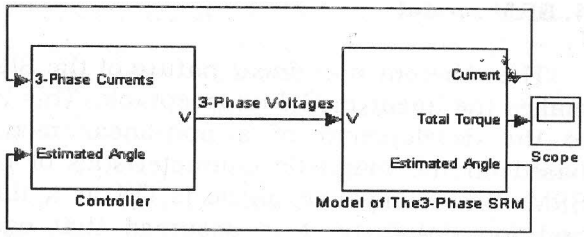

Fig. 9. The complete simulated system.

The 3-Phase model is composed of 3-single phase models combined together in one block with their angle estimator as shown in fig. 9. The estimated angle is fed back to the controller to apply the suitable voltage to the selected phase. Since only one phase is activated at a time hence the mutual inductance is negligible [5].

The motor performance is obtained with and without load.

5.1. System performance at no-load

The motor runs on no-load, only under the inertia of the motor and the friction losses. The DC voltage is set to be 70 V. The speed of the motor was found to be 200 rpm. The current limiter is tuned to 2A. The simulated phase voltage, phase current and the estimated and actual rotor position angle are shown in fig. 10.

Fig. 10 shows that the phase is fired from 45° to 75°, as expected from the pre-computed magnetic characteristics of the motor. The position estimation is shown to be acceptable. The drift at the leading and trailing edges of the position-estimated pulse is due to the interference of the mutual inductance with the successive or preceding phase.

5.2. System performance at load

To get the response of the sensorless motor when it runs under load, a load torque of 0.17 Nm is applied to the motor, this torque is nearly 90% of the rated torque. The voltage is set to 70 V and the current controller is tuned to 2A with a 0.1A hysteresis band. The motor speed was found to be 150 rpm. The simulated phase voltage, phase current and the estimated and actual rotor position angle are shown in fig. 11.

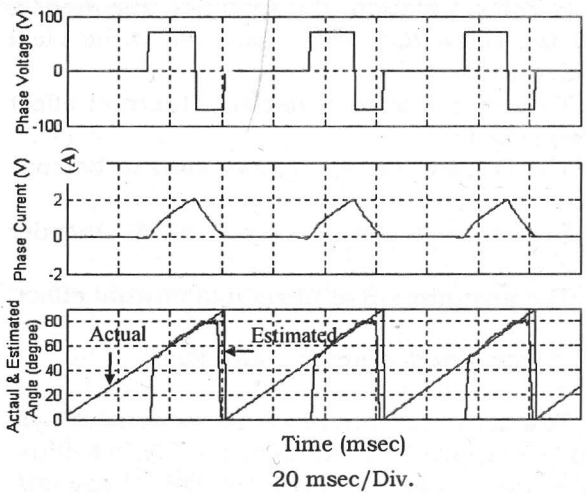

Fig. 10. Simulated phase voltage, current and the estimated and actual rotor angle position.

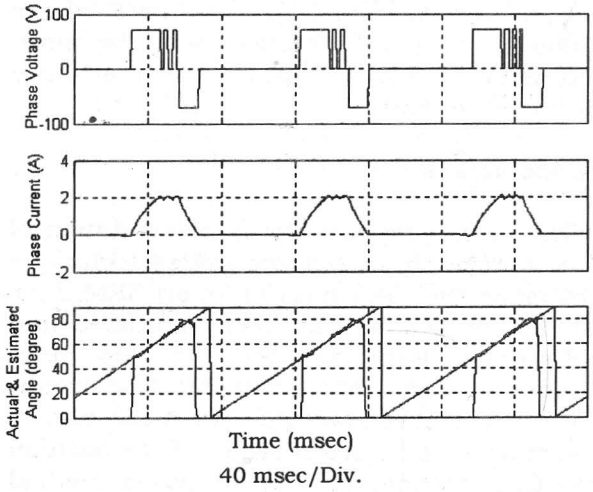

Fig. 11. Simulated phase voltage, current and the estimated and actual rotor angle position.

The lower speed allowed the current to reach its rated value. The current limiter is shown to chop the current to 2A. The Figure shows acceptable position estimation when the motor is loaded. The drift of the estimated position from the actual position became more significant at the trailing edge of the estimated pulse. This is due to the higher values of current in the overlap period between the successive phases. This magnified the mutual effect. The drift is acceptable and can be minimized by taking the mutual effect into account when constructing the lookup tables.

The position estimator gives satisfactory results that fit with the exact position. Neglecting the mutual inductance results in small drift deviation from the exact position at the trailing and leading edges of the position estimated pulse, where the phase is ON while the percussive previous phase is not completely OFF. Adding the mutual inductance effect to the model adds complexity to the system however the benefit is minor.

6. System implementation

The implementation of the proposed sensorless SRM drive system is shown in fig. 12. The PC is selected, because of its flexibility, reliability and availability. The specifications of the PC used in this work are Pentium III 1.1GHz, INTEL microprocessor, 256 KB cache memory and 128 MB RAM. The system adopted here is implemented using two parallel ports of the PC to expand number of I/O's. The first port (input) receives the digital data from the data acquisition card. The second parallel port (output) is used to send the switching pattern to the inverter. The hardware is integrated with a real time Matlab-Simulink written program to achieve the sensorless drive system. Two files were developed in C-language to manage the two parallel ports under the MatLab environment.

A classical inverter topology is used. Each phase is connected to an asymmetric half bridge consisting of two power switches and two diodes. Fig. 13, illustrates the inverter used in this work. The complete DC voltage can be used to energize and de-energize a machine phase in hard chopping mode. When a pair of switches is closed the phase will be energized from the positive DC voltage supply. When both switches are opened, the current commutates through the diodes and rapidly decrease to zero in a negative DC voltage loop. These symmetric half bridges permit soft switching operation, thus obtaining a zero voltage freewheeling state [2].

7. Experimental results

System performances at no load and under load were carried out to evaluate the proposed system.

7.1. System performance at no-load

The system is subjected to the same simulated conditions. Fig. 14 shows the measured phase voltage, phase current and shaft encoder signals. The shaft encoder is used to show that the current pulses and hence the estimated position follows the exact position signal that would be generated from the shaft encoder with acceptable drift margin.

Drift of the simulated results from those carried out experimentally could be due to:

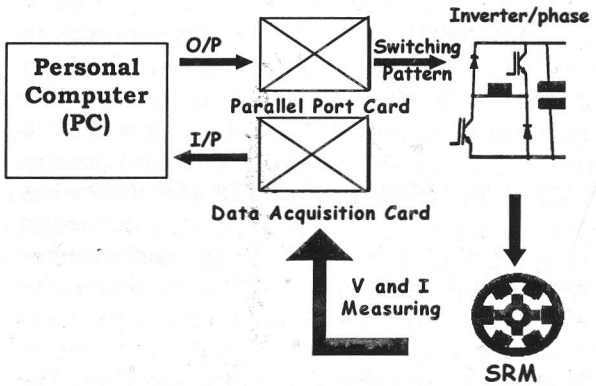

Fig. 12. Block diagram of the implemented system.

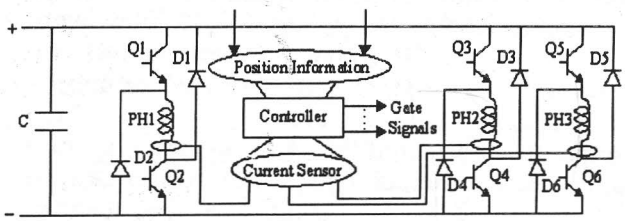

Fig. 13. Inverter circuit topology.

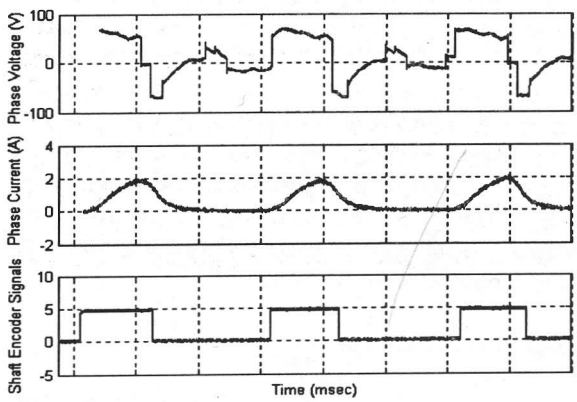

20 msec/Div.

Fig. 14. Experimental phase voltage, current and shaft encoder signals.

- In the simulation, the switches, the diodes, and the capacitors are considered to be ideal elements.
- The error due to resistance thermal effect is neglected.
- The DC link voltage is assessed to be constant.
- Errors in the hand made shaft encoder itself.
- The assumption of negligible mutual effect.

7.2. System performance under load

The same conditions of the simulated system are applied to the system. Fig. 15 illustrates the measured phase voltage, phase current and shaft encoder signals. The experimental results show acceptable performance. The lower speed facilitates more computing time and the estimated position matched the measured position. Differences from the simulated results can be justified by the previously mentioned reasons.

8. Conclusions

This work proposes the implementation of a microprocessor based sensorless technique to estimate the rotor position of an SRM drive system. The system has been simulated and implemented experimentally. It has been evaluated on no load and under load conditions. The simulation and practical results showed acceptable performance of the position estimation technique. This proposed method is low in cost, simple and applicable.

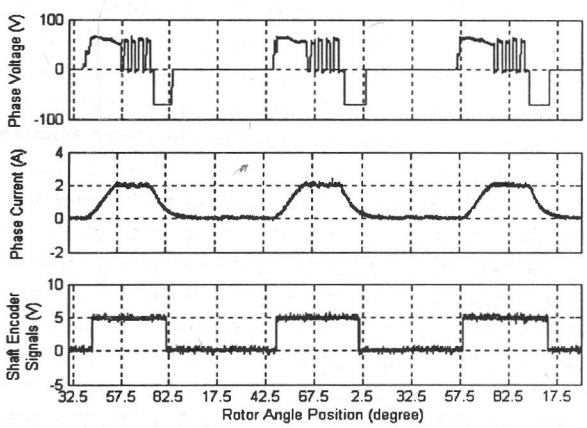

Fig. 15. Experimental phase voltage, current and shaft encoder signals.

References

[1] M. Ehsani, I. Husain, S. Mahajan and K.R. Ramani, "New Modulation Encoding Technique for Indirect Rotor Position Sensing in Switched Reluctance Motors" IEEE Transactions on Industry Applications, Vol. 30 (1), January/ February, pp. 584-588 (1994).

[2] M. Ehsani, I. Husain and A.B. Kulkami, "Elimination of Discrete Position Sensor and Current Sensor in Switched Reluctance Motor Drives", IEEE Transactions on Industry Applications, Vol. 28 (1), January/ February, pp. 128-135 (1992).

[3] J.P. Lyons, S.R. MacMim and M.A. Preston, "Flux/Current Methods for SRM Rotor Position Estimation", IEEE IAS Annual Meeting, pp. 482-487 (1991).

[4] S.R. MacMinn, W.J. Rzesos, P.M. Szczesny and T.M. Jahns, "Application of Sensorless Integration Techniques to Switched Reluctance Motor Drives", IEEE Transactions on Industry Applications, Vol. 28 (6), November/December, pp. 1339-1344 (1992).

[5] Debiprasad Panda and V. Ramanarayanan, "An Accurate Position Estimation Method for Switched Reluctance Motor Drive", International Conference on Power Electronics Drives and Energy Systems (PEDES'98), Perth, Australia, December, pp. 523-528 (1998).

[6] W.D. Harris and J.H. Lang, "A Simple Motion Estimator for Variable Reluctance Motors", IEEE Transactions on Industry Applications, Vol. 26 (2), March/April, pp. 237-243 (1990).

[7] A. Lumsdaine and J.H. Lang, "State Observers for Variable Reluctance Motors", IEEE Transactions on Industrial Electronics, Vol. 37 (2), pp. 133-142, (1990).

[8] A. Brosse and G. Hennerberger, "Sensorless Control of SRM Drives with Kalman Filter Approach", EPE Conference Records, 7th European Conference on Power Electronics and Applications, Trondheim, Norway, 8-10 September, pp. 2.500-2.505 (1997).

[9] A. Brosse, G. Hermeberger, M. Schniedemeyer, R.D. Lorenz and N. Nagel, "Sensorless Control of a SRM at Low Speeds and Standstill Based on Signal Power Measurement", IEEE IECON Conference Records, pp. 1538-1543 (1998).

[10] G. Suresh, B. Fahimi, K.M. Rahman and M. Ehsani, "Inductance Based Position Encoding for Sensorless SRM Drives", IEEE IAS (Industry Applications Society) Annual Meeting, Vol. 2, pp. 100-105 (1999).

[11] D. Reay and B.W. Williams, "Sensorless Position Detection Using Neural Networks for the Control of Switched Reluctance Motors," Proceedings of the IEEE International conference on control applications, Vol. 2, pp. 1073-1077 (1999).

[12] A. Cheek and N. Ertugrul, "A Model Fuzzy Logic Based Rotor Position Sensorless Switched Reluctance Motor Drives", IEEE-IAS (Industry Applications Society), Annual Meeting, Vol. 1, pp. 76-83 (1996).

Received January 19, 2005
Accepted July 30, 2005